

Laboratory Observation of a Nonlinear Interaction between Shear Alfvén Waves

T. A. Carter,^{1,2,*} B. Brugman,^{1,2} P. Pribyl,¹ and W. Lybarger¹

¹*Department of Physics and Astronomy, University of California, Los Angeles, California 90095-1547, USA*

²*Center for Multiscale Plasma Dynamics, University of California, Los Angeles, California 90095-1547, USA*

(Received 22 September 2005; published 21 April 2006)

An experimental investigation of nonlinear interactions between shear Alfvén waves in a laboratory plasma is presented. Two Alfvén waves, generated by a resonant cavity, are observed to beat together, driving a pseudomode at the beat frequency. The pseudomode then scatters the Alfvén waves, generating a series of sidebands. The observed interaction is very strong, with the normalized amplitude of the driven pseudomode comparable to the normalized magnetic field amplitude ($\delta B/B$) of the interacting Alfvén waves.

DOI: [10.1103/PhysRevLett.96.155001](https://doi.org/10.1103/PhysRevLett.96.155001)

PACS numbers: 52.35.Bj, 52.35.Mw

The Alfvén wave is the fundamental low-frequency normal mode of a magnetized plasma and is important both in space plasmas [e.g., the auroral ionosphere [1], the solar wind [2]] and in laboratory plasmas [e.g., tokamaks [3] and linear devices [4]]. From a weak turbulence point of view, nonlinear interactions between Alfvén waves are responsible for the cascade of energy in magneto-hydrodynamic (MHD) turbulence [5]. In the incompressible MHD approximation, only counterpropagating shear Alfvén waves can interact, and these interactions lead to an anisotropic energy cascade [6]. With the inclusion of non-ideal effects such as finite ion gyroradius ($k_{\perp}\rho_s \sim 1$, where ρ_s is the ion gyroradius based on the sound speed), finite skin depth ($k_{\perp}\delta_e \sim 1$, where $\delta_e = c/\omega_{pe}$ is the electron skin depth), and finite frequency ($\omega/\omega_{c,i} \sim 1$, where $\omega_{c,i}$ is the ion cyclotron frequency), shear Alfvén waves become the dispersive inertial and kinetic Alfvén waves [7]. In laboratory plasmas, mode-converted kinetic Alfvén waves are thought to be important in radio frequency (rf) heating experiments [8,9] and in the damping of Alfvén eigenmodes [10]. In space plasmas, dispersive Alfvén waves are invoked to explain particle acceleration [11], ponderomotive density modification [12], and heating [13]. For dispersive Alfvén waves, both counter and copropagating wave packets can interact nonlinearly [14], and lone wave packets can suffer decay instabilities. These instabilities include the parametric [15,16] and modulational [17,18] decay instabilities, where the pump and daughter Alfvén waves beat together to drive an ion acoustic wave and a nonlinear pseudomode, respectively.

In this Letter, an observation of a nonlinear interaction between shear Alfvén waves in a laboratory plasma is presented. While nonlinear interactions between Alfvén waves have been previously reported in high-power radio frequency heating experiments in magnetic confinement fusion devices [19], the experiments reported here represent the first controlled study of nonlinear wave-wave interactions with detailed measurements of spatial structure. In addition, these experiments are the first to investigate nonlinear interactions between kinetic Alfvén

waves. Large amplitude shear Alfvén waves are generated using a resonant cavity. In circumstances where two waves are simultaneously emitted by the cavity, production of sideband Alfvén waves and fluctuations at the sideband separation frequency is observed. The interaction is identified as a beat-wave interaction between copropagating shear waves, where a nonlinear pseudomode is driven at the beat frequency. The pseudomode represents a driven oscillation and does not correspond to a linear normal mode of the plasma but effectively scatters the pump Alfvén waves, generating a spectrum of Alfvénic sidebands. Strong parametric excitation of nonlinear pseudomodes, also called nonresonant ion quasimodes, by ion cyclotron waves has also been observed experimentally [20].

The experiments were performed in the upgraded Large Plasma Device (LAPD) which is part of the Basic Plasma Science Facility (BAPSF) at UCLA [21]. LAPD is an 18 m long, 1 m diameter cylindrical vacuum chamber, surrounded by 90 magnetic field coils. Pulsed plasmas (~ 10 ms in duration) are created at a repetition rate of 1 Hz using a barium oxide coated nickel cathode source. A discharge current (typically ~ 5 kA) flows between the cathode and a semitransparent anode located 0.55 m away, generating a beam of primary electrons (typical energy 50 eV) which enter the main column, ionizing and heating the fill gas. The main LAPD plasma column is current free, with the current due to the injected primary electrons balanced by a back-drifting population of thermal electrons [22]. Typical plasma parameters are $n_e \sim 1 \times 10^{12}$ cm⁻³, $T_e \sim 6$ eV, $T_i \sim 1$ eV, and $B < 2$ kG and the experiments are performed using helium as a working gas. In these experiments, $\beta \gtrsim m_e/M_i$, and the electron thermal speed is therefore larger than the Alfvén speed. This fact, coupled with finite $k_{\perp}\rho_s$ (here $\rho_s \sim 0.5$ – 1.5 cm), makes the Alfvén waves in these experiments dispersive kinetic Alfvén waves [7]. Additional dispersive effects arise due to finite $\omega/\omega_{c,i}$.

Large amplitude shear Alfvén waves are generated using the Alfvén wave maser [22,23]. The cathode and semitransparent anode of the plasma source define a resonant

cavity from which spontaneous shear wave emission with $f \sim 0.6f_{ci}$ and $k_{\perp}\rho_s \sim 0.3\text{--}0.5$ is observed. The emitted waves are eigenmodes [24] of the cylindrical LAPD plasma column, with $m = 0$ or $m = 1$ azimuthal mode number. The modes are left-hand polarized [22], and here we use the convention where positive m numbers indicate that polarization. The amplitude of the waves can be large, $\delta B/B \geq 1\%$, and may be controlled through changing the plasma source discharge current. Strong nonlinear effects can be expected when the field line displacement in the wave is comparable to the perpendicular wavelength ($\delta B/B \geq k_{\parallel}/k_{\perp}$) [6], a condition which is satisfied for these waves ($k_{\parallel}/k_{\perp} \sim 1\%\text{--}4\%$).

Figure 1(a) shows the fast Fourier transform (FFT) power spectrum versus time for magnetic field fluctuations measured in the main LAPD plasma column (~ 7 m from the source region). Figure 1(b) shows a line plot of the spectrum at $t = 8$ ms at which point the discharge and plasma column have reached steady state (helium discharge, 700 G, $f_{ci} = 266$ kHz). Maser emission begins early in the LAPD discharge, as the source region current is ramping up and plasma parameters and profiles are evolving. During this early phase ($t \lesssim 6$ ms) the emission is observed to “mode hop” [23] with the second hop identified through mode structure measurements as a transition from $m = 0$ to $m = 1$. After the mode hop, the $m = 0$ mode does not disappear, but persists at a much lower level. An additional frequency is observed in the spectrum, located above the $m = 1$ frequency by the difference frequency between the $m = 0$ and $m = 1$ modes. This mode appears to be a sideband of the primary $m = 1$

mode which is generated by a weak nonlinear interaction between the $m = 0$ and $m = 1$ mode.

Much stronger sideband generation is observed during high-current discharges when the length of the main LAPD plasma column is shortened to 10 m by terminating the plasma with an electrically floating aluminum plate. Figures 1(c)–1(f) show FFT power spectra of measured magnetic field (B) and Langmuir probe measured ion saturation current (I_{sat}) during maser emission with a terminated column. The magnetic spectrum is considerably more complicated in this case, showing fluctuations at a number of discrete frequencies. In the steady state phase of the discharge ($t > 6$ ms), there are two strong modes present (identified as $m = 0$ and $m = 1$), surrounded by a number of sidebands. Simultaneously, I_{sat} fluctuations are observed at the sideband separation frequency and harmonics. These observations are consistent with the following scenario. (1) Two large amplitude shear modes (e.g., $m = 1$ and $m = 0$) of differing frequency are simultaneously emitted from the cavity. (2) Because of dispersion, the two copropagating waves have slightly different phase velocities, allowing them to pass through one another and beat together, driving a fluctuation at the beat frequency. (3) The driven fluctuation then scatters the incident shear waves, leading to sideband generation. Our conjecture is that the termination of the plasma column at high discharge current induces simultaneous emis-

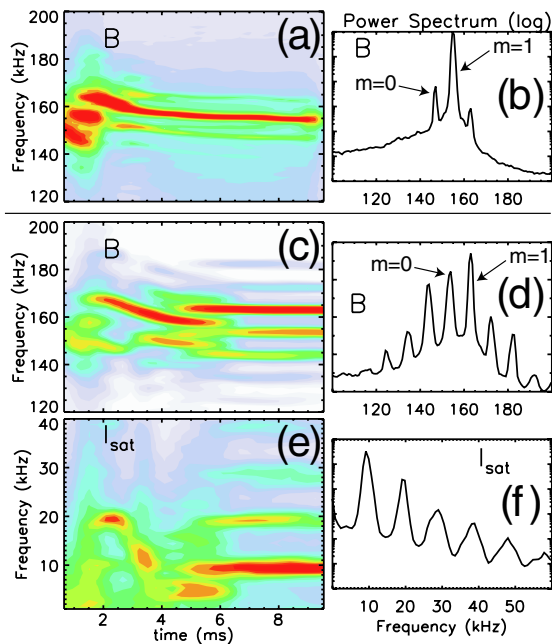


FIG. 1 (color online). (a), (b): Typical power spectrum of shear Alfvén waves during maser emission. Bottom: B [(c), (d)] and I_{sat} [(e), (f)] power spectra during maser emission with floating-plate termination.

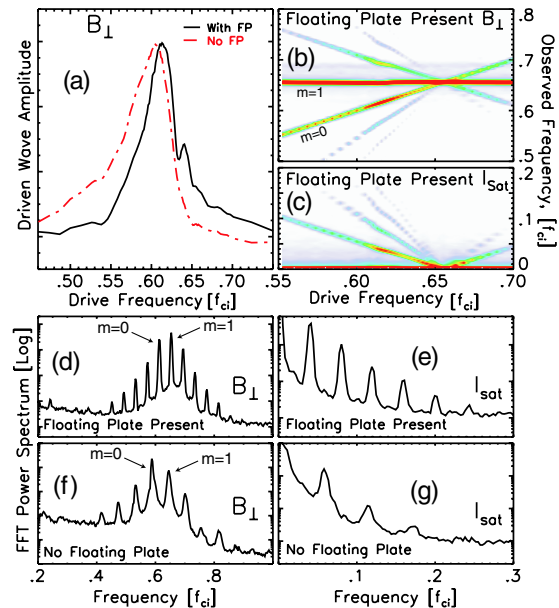


FIG. 2 (color online). (a) Cavity response as a function of normalized external drive frequency. (b) Magnetic power spectrum and (c) I_{sat} power spectrum due to interacting shear waves during a frequency separation scan. For drive frequency on the $m = 0$ resonance: (d) magnetic power spectrum and (e) ion saturation current spectrum with the floating-plate present. (f) Magnetic power spectrum and (g) I_{sat} power spectrum without the floating plate.

sion of large amplitude $m = 0$ and $m = 1$ modes, leading to the proposed scenario.

In order to test this conjecture, the capability to externally drive the resonant cavity has been developed. To excite the cavity, oscillating currents are driven between the anode and cathode using external power supplies. Figure 2(a) shows the cavity response (magnitude of the emitted wave, measured in the main plasma column) as a function of drive frequency (normalized to f_{ci}) for cases with and without the floating plate present. The resonant nature of the cavity emission is clear, as is the modification in the emission properties of the cavity by shortening the column using the floating plate. The external drive couples primarily to the $m = 0$ mode, but the additional peak observed with the floating plate present corresponds to the $m = 1$ mode frequency, and may indicate coupling to that mode. The cavity was operated so that the spontaneous emission of only one mode ($m = 1$) is observed, and a second mode ($m = 0$) was externally excited. This allows for a controlled investigation of the interaction between the two Alfvén waves with a variable separation frequency.

Figures 2(b) and 2(c) show the transverse magnetic (B_{\perp}) and I_{sat} power spectrum versus drive frequency during a frequency separation scan with the floating plate present. The spontaneous emission ($m = 1$) is fixed during the scan (the horizontal feature at $f \sim 0.66f_{ci}$ in B_{\perp}) while the frequency of the driven mode is changed from shot to shot. The production of sidebands, in particular, the first upper sideband, is evident over a wide range of frequency separations between the driven ($m = 0$) and spontaneous ($m = 1$) waves as is the generation of I_{sat} perturbations at the difference frequency and its harmonics. The change in sideband amplitude versus frequency separation is primarily due to changes in the externally driven mode amplitude with frequency (due to the Q of the cavity). Figure 2(d) shows a line plot of the magnetic power spectrum when the drive frequency is at the peak of the $m = 0$ resonance, $f_{\text{drive}} = 0.61f_{ci}$. A number of sidebands around the driven ($m = 0$) and spontaneous ($m = 1$) shear waves are visible. Figure 2(e) shows the I_{sat} power spectrum at the same drive frequency, which exhibits fluctuations at the sideband separation frequency and harmonics. Figures 2(f) and 2(g) show B_{\perp} and I_{sat} spectra from interaction experiments without the floating plate present. Shifts in the absolute frequency and frequency separation of the $m = 0$ and $m = 1$ modes are evident relative to the case with the floating plate present due to changes in plasma parameters. Aside from these differences in the cavity response, the spectra observed without the floating plate are quite similar to those observed with the floating plate: magnetic sidebands are evident, as are I_{sat} fluctuations at the sideband separation frequency. This suggests that the primary role of floating-plate termination in the data shown in Fig. 1 is to modify the cavity properties so that two large amplitude shear wave modes are emitted simultaneously. The mechanism by which the floating plate causes this spontaneous multimode emission is not yet understood, but it is known

that plasma parameters and profiles are altered relative to the nonterminated case. The presence of the floating plate also defines a second resonant cavity and through reflections allows for the possibility of a counterpropagating population of the Alfvén waves. However, the qualitative similarity between the cases with and without the floating plate shown in Fig. 2 suggests that the second cavity and the associated reflected waves are not essential for the interaction, and that instead the observed interaction is between copropagating shear waves.

Figure 3 shows the structure of the fluctuations during an interaction between driven ($m = 0$) and spontaneously emitted ($m = 1$) cavity shear modes. Because of the shot-to-shot phase variation in the spontaneous emission, cross-correlation techniques are used to determine the structure of the interacting modes. Two probes are used, one fixed at a spatial location (to provide a phase reference) while the second, 1 m away axially, is moved shot to shot to 961 positions in the plane perpendicular to the background field. Figure 3 shows the driven maser wave has an $m = 0$ structure, with a hollow amplitude profile and a single current channel. The spontaneous maser exhibits primarily an $m = 1$ structure, with two counterrotating current channels and a peaked amplitude profile between the two. The structure of the nonlinearly generated upper sideband has some similarity to the spontaneous $m = 1$ emission, but is more concentrated in the periphery, which may be consistent with $m > 1$ mode content. The pattern of the I_{sat} fluctuation is more centrally localized, but is not readily identifiable as a single azimuthal mode number. If a three-wave process were to explain the observations, three-wave matching rules would predict $m = 1$ for the low-frequency mode and $m = 2$ for the upper sideband. Differences between the observations and these predictions could be

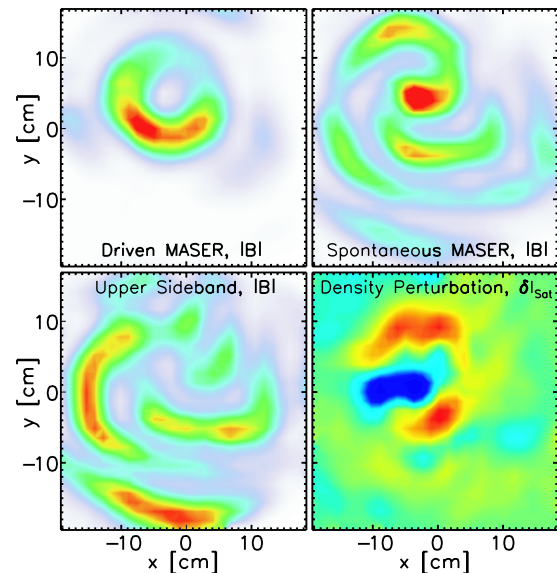


FIG. 3 (color online). Structure of the driven maser, spontaneous maser, upper sideband, and low frequency I_{sat} fluctuation in the plane perpendicular to B .

explained by density inhomogeneity in the plane perpendicular to \mathbf{B} or by effects from higher-order processes (e.g., four-wave interactions). These possibilities will be investigated in future work. Experiments were also performed where two $m = 0$ modes were driven in the absence of spontaneous maser emission. The two modes were driven slightly off resonance in order to obtain a frequency (and phase velocity) separation. Driven low-frequency fluctuations and Alfvén wave sideband generation consistent with the previous results are also observed in this case, indicating that the interaction is not dependent on the two interacting waves possessing different transverse mode numbers. In this case, the nonlinearly driven modes are observed to possess a $m = 0$ perpendicular structure, consistent with three-wave matching.

The parallel phase velocity of the low-frequency mode was measured during the experiments with two driven $m = 0$ modes using probe pairs separated by 2.88 m along the magnetic field. The average parallel phase velocity was measured to be 294 ± 35 km/s, where the Alfvén speed was ~ 550 km/s and the ion acoustic speed was ~ 13 km/s. A velocity of 291 km/s is calculated using the three-wave matching rules between the upper and lower launch wave and the density perturbation and the kinetic Alfvén wave dispersion relation, $\omega^2 = k_{\parallel}^2 v_A^2 (1 - \omega^2/\Omega_{ci}^2 + k_{\perp}^2 \rho_s^2)$. Although the two interacting waves are cylindrical eigenmodes, the plane wave dispersion relation is appropriate provided that k_{\perp} is defined by the argument of the Bessel function describing the radial mode structure [24]. A spatial fit of the measured $m = 0$ mode structure gives $k_{\perp} \rho_s \sim 0.38$ [23]. The phase velocity measurement shows that the low-frequency fluctuation is consistent with a three-wave process and also that it does not correspond to a linear plasma wave (e.g., an ion acoustic wave) and is instead a driven nonlinear perturbation or pseudomode.

The amplitude of the I_{sat} fluctuation is observed to scale roughly bilinearly with the amplitude of the two interacting shear waves. The normalized amplitude of the I_{sat} fluctuations is quite large with $\delta I_{\text{sat}}/I_{\text{sat}} \sim 1\% - 10\% \gtrsim \delta B/B$. In addition to density, I_{sat} measured by a probe is sensitive to electron temperature, potential fluctuations, and any population of fast electrons (those with energies greater than the negative probe bias ~ 65 V). Therefore, fluctuations in these quantities could contribute to the magnitude of observed I_{sat} signal. Preliminary microwave interferometer measurements indicate that significant line-average density fluctuations associated with the pseudomode are present. Future work will focus on measurements which accurately determine the magnitude of $\delta n/n$ in the pseudomode. More comprehensive theoretical predictions, in particular, incorporating nonideal effects associated with finite $\omega/\omega_{c,i}$ and $k_{\perp} \rho_s$, will be required to determine whether the beat-wave drive can generate the observed large amplitude density fluctuations.

In summary, a nonlinear beat-wave interaction between shear Alfvén waves has been observed. Two resonant-cavity-produced, copropagating shear waves are observed to beat together, resulting in a low-frequency fluctuation at the beat frequency and the subsequent creation of Alfvénic sidebands. The low-frequency fluctuation is identified as a nonlinearly driven pseudomode generated by the beat between the two copropagating shear waves. While the observations are not consistent with a decay instability, it should be pointed out that pseudomode production by copropagating Alfvén waves occurs during modulational decay [18]. Counterpropagating interactions will be explored in future experiments, where beat-wave driven ion acoustic waves may be possible. The relevance of the interaction between cylindrical eigenmodes to plane wave interactions and space observations is a key question which will be addressed in future work.

The authors would like to thank S. Cowley, W. Gekelman, G. Morales, and J. Maggs for invaluable discussions. This work was completed using the Basic Plasma Science Facility at UCLA, which is funded by DOE and NSF. This work was supported by DOE Grant No. DE-FG02-02ER54688 and by DOE Fusion Science Center Cooperative Agreement No. DE-FC02-04ER54785.

*Electronic address: tcarter@physics.ucla.edu

- [1] D. A. Gurnett *et al.*, *J. Geophys. Res.* **89**, 8971 (1984).
- [2] J. W. Belcher *et al.*, *J. Geophys. Res.* **74**, 2302 (1969).
- [3] W. W. Heidbrink *et al.*, *Phys. Rev. Lett.* **71**, 855 (1993).
- [4] W. Gekelman *et al.*, *Phys. Plasmas* **1**, 3775 (1994).
- [5] R. Kraichnan, *Phys. Fluids* **8**, 1385 (1965).
- [6] P. Goldreich and S. Sridhar, *Astrophys. J.* **485**, 680 (1997).
- [7] S. Vincena *et al.*, *Phys. Rev. Lett.* **93**, 105003 (2004).
- [8] A. Hasegawa and L. Chen, *Phys. Fluids* **19**, 1924 (1976).
- [9] H. Weisen *et al.*, *Phys. Rev. Lett.* **63**, 2476 (1989).
- [10] G. Y. Fu *et al.*, *Phys. Plasmas* **12**, 082505 (2005).
- [11] C. A. Kletzing and S. Hu, *J. Geophys. Res.* **99**, 693 (1994).
- [12] B. Dasgupta *et al.*, *Geophys. Res. Lett.* **30**, 2128 (2003).
- [13] A. Hasegawa and L. Chen, *Phys. Rev. Lett.* **35**, 370 (1975).
- [14] Y. M. Voitenko, *J. Plasma Phys.* **60**, 497 (1998).
- [15] A. Hasegawa and L. Chen, *Phys. Rev. Lett.* **36**, 1362 (1976).
- [16] S. Spangler *et al.*, *Phys. Plasmas* **4**, 846 (1997).
- [17] H. Wong and M. Goldstein, *J. Geophys. Res.* **91**, 5617 (1986).
- [18] J. V. Hollweg, *J. Geophys. Res.* **99**, 23 431 (1994).
- [19] G. G. Borg *et al.*, *Nucl. Fusion* **33**, 841 (1993).
- [20] M. Ono *et al.*, *Phys. Fluids* **23**, 1675 (1980).
- [21] W. Gekelman, <http://plasma.physics.ucla.edu/bapsf>.
- [22] J. E. Maggs and G. J. Morales, *Phys. Rev. Lett.* **91**, 035004 (2003).
- [23] J. E. Maggs *et al.*, *Phys. Plasmas* **12**, 013103 (2005).
- [24] L. C. Woods, *J. Fluid Mech.* **13**, 570 (1962).